Giant room-temperature electrostrictive coefficients in lead-free relaxor ferroelectric ceramics by compositional tuning

Aman Ullah, Hafiza Bushra Gul, Amir Ullah, Muhammad Sheeraz, Jong-Seong Bae, Wook Jo, Chang Won Ahn, Ill Won Kim, and Tae Heon Kim

Citation: APL Materials **6**, 016104 (2018);
View online: https://doi.org/10.1063/1.5006732
View Table of Contents: http://aip.scitation.org/toc/apm/6/1
Published by the American Institute of Physics

Giant room-temperature electrostrictive coefficients in lead-free relaxor ferroelectric ceramics by compositional tuning

Aman Ullah,[1,2] Hafiza Bushra Gul,[2] Amir Ullah,[3] Muhammad Sheeraz,[1] Jong-Seong Bae,[4] Wook Jo,[5] Chang Won Ahn,[1] Ill Won Kim,[1,a] and Tae Heon Kim[1,a]

[1]*Department of Physics and Energy Harvest Storage Research Center (EHSRC), University of Ulsan, Ulsan 44610, South Korea*
[2]*Department of Physics, University of Science and Technology, Bannu, Khyber Pakhtunkhwa, Pakistan*
[3]*Department of Physics, Islamia College, Peshawar, Khyber Pakhtunkhwa, Pakistan*
[4]*Busan Center, Korea Basic Science Institute, Busan 46742, South Korea*
[5]*School of Materials Science and Engineering, Ulsan National Institute of Science and Technology, UNIST, Ulsan 44919, South Korea*

(Received 27 September 2017; accepted 20 December 2017; published online 16 January 2018)

A thermotropic phase boundary between non-ergodic and ergodic relaxor phases is tuned in lead-free $Bi_{1/2}Na_{1/2}TiO_3$-based ceramics through a structural transition driven by compositional modification (usually named as "morphotropic approach"). The substitution of $Bi(Ni_{1/2}Ti_{1/2})O_3$ for $Bi_{1/2}(Na_{0.78}K_{0.22})_{1/2}TiO_3$ induces a transition from tetragonal to "metrically" cubic phase and thereby, the ergodic relaxor ferroelectric phase becomes predominant at room temperature. A shift of the transition temperature (denoted as $T_{F\text{-}R}$) in the non-ergodic-to-ergodic phase transition is corroborated via temperature-dependent dielectric permittivity and loss measurements. By monitoring the chemical composition dependence of polarization-electric field and strain-electric field hysteresis loops, it is possible to track the critical concentration of $Bi(Ni_{1/2}Ti_{1/2})O_3$ where the $(1-x)Bi_{0.5}(Na_{0.78}K_{0.22})_{0.5}TiO_3$-$xBi(Ni_{0.5}Ti_{0.5})O_3$ ceramic undergoes the phase transition around room temperature. At the $Bi(Ni_{0.5}Ti_{0.5})O_3$ content of $x = 0.050$, the highest room-temperature electrostrictive coefficient of 0.030 m^4/C^2 is achieved with no hysteretic characteristic, which can foster the realization of actual electrostrictive devices with high operational efficiency at room temperature. https://doi.org/10.1063/1.5006732

Electrostriction, where electric-field-induced strain (S_{33} in the out-of-plane direction) is proportional to the square of out-of-plane polarization (P_3) (i.e. $S_{33} = Q_{33} \cdot {P_3}^2$, Q_{33} stands for an electrostriction coefficient), is of a practical interest in aspect of device applications to micro-electromechanical systems (MEMS).[1] Unlike piezoelectricity with a linear electromechanical coefficient, an electrostrictive effect has been known to possess a large variety of technological benefits/advantages for realizing novel MEMS devices, such as little hysteretic characteristics in the electromechanical responses, good thermal stability, a short operational time, and no need of a poling process.[1–4] In conventional relaxor ferroelectrics (FEs) belonging to the family of lead-based complex oxides, high S_{33} of 0.1% and a large Q_{33} value of 0.02 m^4/C^2 have been realized at room temperature.[4–7] However, due to strict regulations of lead-based compounds for global environment,[3] a comparable electrostrictive response should be achieved in lead-free compounds for their eco-friendly and sustainable utilization. Furthermore, for potential applications to actual devices, it may be also accessible at room temperature.

[a]Authors to whom correspondence should be addressed: thkim79@ulsan.ac.kr and kimiw@ulsan.ac.kr

$Bi_{0.5}Na_{0.5}TiO_3$ (BNT)-based relaxor FEs are an excellent class of lead-free oxide materials for realizing high electrostrictive responses.[4,8–16] We notice that an ultrahigh electrostrictive coefficient is attainable in the vicinity of a thermotropic phase boundary which is a thermally-induced boundary between two competing phases [i.e., ergodic relaxor (ER) and non-ergodic relaxor (NR) phases in BNT-based materials].[16,17] In an ergodic phase above a transition temperature ($T_{F\text{-}R}$), a relaxor FE state, with macroscopic paraelectricity, where the crystallographic symmetry is metrically cubic, is reversibly converted to an FE state by the application of an external electric field. In contrast, for a non-ergodic phase below $T_{F\text{-}R}$, the FE state induced by a sufficiently large electric field is irreversible.[16,17] Near the phase boundary between the ER and NR phases, large net strain and relatively small remnant polarization values under an external electric field are feasible with little polarization-electric field hysteresis, which enables a nearly pure electrostrictive response with a large Q_{33} value ($\sim S_{33}/{P_3}^2$) (see Fig. S1 of the supplementary material).[8] Since the $T_{F\text{-}R}$ of this NR-to-ER phase transition is commonly higher than room temperature [e.g., the $T_{F\text{-}R}$ of $Bi_{0.5}(Na_{0.78}K_{0.22})_{0.5}TiO_3$ (BNKT) ceramics is about 150 °C],[18] tuning the $T_{F\text{-}R}$ towards room temperature is essential for us to achieve a large room-temperature electrostrictive coefficient in BNT-based relaxor FEs.[9]

Recently, it has been expected that the transition temperature of $T_{F\text{-}R}$ in BNT-based ceramics can be reduced by modifying the chemical composition of the parent compound.[9,13,18–20] Besides, the $T_{F–R}$ can be tuned by the external electric field.[21] Note that bulk BNKT undergoes a NR-to-ER phase transition around ∼150 °C and the degree of FE order is also susceptible to slight changes in the cation content. It is, therefore, possible that the transition temperature in BNKT ceramics can be manipulated, when a room-temperature tetragonal phase is converted to a metrically cubic phase by stoichiometry control.[13,18–20] It is further interesting that an exceptionally high electrostrictive coefficient could appear at room temperature, if the BNKT composite undergoes a NR-to-ER phase transition nearby room temperature.[9]

In this work, compositional tuning of $T_{F\text{-}R}$ is implemented to design a new BNT-based material with an ultrahigh room-temperature electrostrictive coefficient. To assess our synthetic approach, Bi-based $Bi_{0.5}(Na_{0.78}K_{0.22})_{0.5}TiO_3$ (BNKT) and $Bi(Ni_{0.5}Ti_{0.5})O_3$ (BNiT) are selected as a base compound and a chemical modifier, respectively.[21–23] Note that multi-charge valency is accessible in these transition-metal Ni and Ti cations and also, their ionic radiuses are sensitive to the oxidation states.[24] By substituting the BNiT for the BNKT, the initial tetragonal structure would change with a pseudocubic (metrically cubic) distortion, probably due to the different ionic radius between competing B-site cations.[18,21,23,24] Thus, the transition temperature $T_{F\text{-}R}$ between non-ergodic and ergodic phases can be shifted towards room temperature.[25] By measuring temperature-dependent dielectric responses in the BNKT-BNiT composite, a shift of the $T_{F\text{-}R}$ by compositional modification is clearly demonstrated. A giant room-temperature electrostrictive coefficient is also recorded in the BNKT-BNiT ceramic with a particular BNiT content. The reduction of the $T_{F\text{-}R}$ to room temperature allows large strain available, *albeit* polarization is relatively small, leading to an enhancement in the room-temperature electrostrictive coefficient.

High-quality $(1-x)$BNKT-xBNiT ceramics, where x varies from 0.0 to 0.100, were synthesized using solid state reaction method (see the supplementary material for detail). All $(1-x)$BNKT-xBNiT samples were densely synthesized with no impurity/pore on the sample surface implying that the chemical stoichiometry is spatially homogeneous and the incorporated elements are well coalesced (see Fig. S2 of the supplementary material).

To check the crystallinity of our $(1-x)$BNKT-xBNiT compounds, we performed x-ray diffraction (XRD) θ-2θ scans of our samples in the 2θ range of 20°-80° (see Fig. S3 of the supplementary material), it was identified that the ceramic samples are a perovskite single phase without any secondary phase. Figure 1(a) of the XRD θ-2θ scans in the narrow range of 35°-50° shows that the crystallographic structure evolves, as the mole concentration of BNiT (x) increases. In the pure BNKT ($x = 0.0$) with a tetragonal symmetry, the Bragg (002) and (200) peaks around 46.5° are split due to the different out-of-plane d-spacings of c and a domains, whereas the multi-domain state of $c + a$ is indistinguishable in the Bragg (111) peak around 40.0°. It is interesting that the observed splitting in the (002)/(200) peak disappears with the increasing x and finally, the peak becomes single when the x value is 0.040. In contrast, the (111) peak remains roughly unchanged with respect to

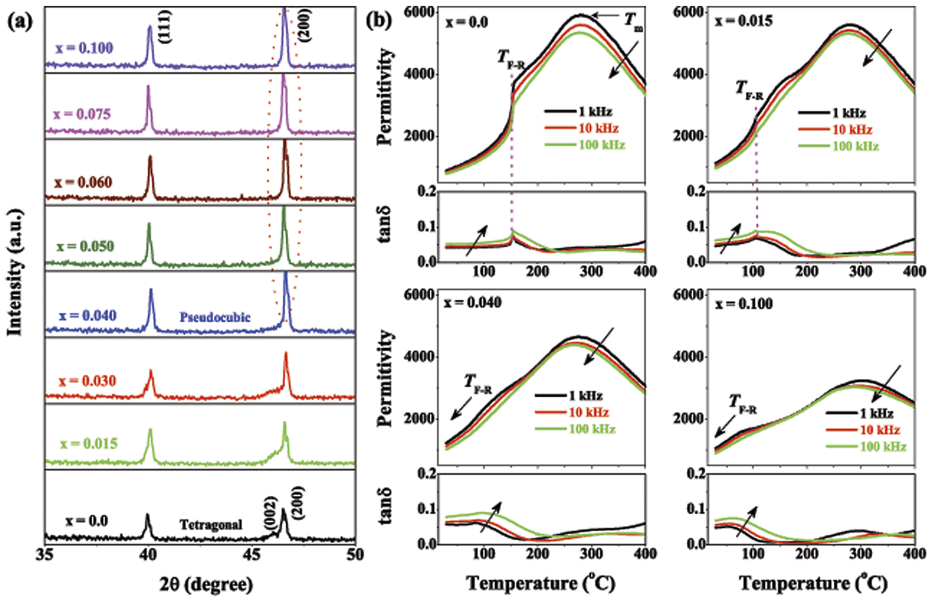

FIG. 1. (a) XRD patterns of $(1 - x)$BNKT-xBNiT ceramics, acquired over the 2θ range of 35°–50° (b) frequency and temperature dependence of the dielectric properties of poled $(1 - x)$BNKT-xBNiT ceramics (x = 0.0, 0.015, 0.040, and 0.100).

all x values. Note that the spectral shapes/patterns of these (002)/(200) and (111) peaks are strongly dependent on the crystallographic symmetry of the BNT-based materials (see Fig. S4 of the supplementary material). When the tetragonal symmetry approaches a metrically cubic, the (002)/(200) and (111) peaks get closer to single without a peak separation. It follows that our $(1 - x)$BNKT-xBNiT ceramics undergo a tetragonal-to-metrically cubic structural transition with the increasing concentration of BNiT inducing changes in the spectra of the x-ray Bragg peaks. In $(1 - x)PbTiO_3$-xBNiT ceramics with divalent Ni^{2+} cation which disfavors the hybridization with an oxygen atom and thus, promotes the stability of a pseudocubic phase, a similar tetragonal-to-pseudocubic transition has been reported.[26,27] To confirm the oxidation state of Ni, x-ray photoelectron spectroscopy (XPS) analysis of $(1 - x)$BNKT-xBNiT (x = 0, 0.050, and 0.100) compounds was performed (see Fig. S5 of the supplementary material). The XPS spectra at Ni $2p_{3/2}$ peak shows that divalent Ni^{2+} and metallic Ni states coexist at the binding energy of ~855.08 and 852.58 eV, respectively. Thus, Ni cation with a charge valence of +2 (i.e., Ni^{2+}) is solely substituted for quadrivalent Ti^{4+} in the BNKT compound.[28–31]

Temperature-dependent dielectric measurements in our $(1 - x)$BNKT-xBNiT ceramics reveal that the transition temperature $T_{F\text{-}R}$ of a NR-to-ER transition is shifted towards room temperature, due to the tetragonal-to-pseudocubic phase transition. The temperature dependence of dielectric permittivity and loss (tan δ) was measured under the various ac frequencies of 1, 10, and 100 kHz [Fig. 1(b)]. It is evident that the transition temperature $T_{F\text{-}R}$ (indicated by red dotted lines), where anomalies in both dielectric permittivity and loss appear, changes from 150 to 104 °C, as the x value increases from 0.0 to 0.015, respectively. With a further increase (≥0.040) in the BNiT concentration x, the $T_{F\text{-}R}$ vanishes eventually. Since our dielectric measurements have been done in the temperature range of 30–400 °C, it is highly likely that the $T_{F\text{-}R}$ is shifted below room temperature. Considering the fact that the structural symmetry of our $(1 - x)$BNKT-xBNiT ceramics is transformed from tetragonal to metrically cubic above x = 0.040, the movement of the $T_{F\text{-}R}$ across room temperature would be closely related with this structural transition. Such shift of the $T_{F\text{-}R}$ in dielectric dispersion behaviors by structural changes has been previously reported in other BNT-based relaxor FEs.[11,18,20,32–34]

To get a further insight into the compositionally-induced shift of $T_{F\text{-}R}$, room-temperature polarization-electric field (P_3-E) and bipolar strain-electric field (S_{33}-E) hysteresis loops of our $(1 - x)$BNKT-xBNiT ceramics were measured as shown in Figs. 2(a) and 2(b), respectively. As the BNiT content x increases, three types of hysteretic behaviors are observed. For a pure BNKT

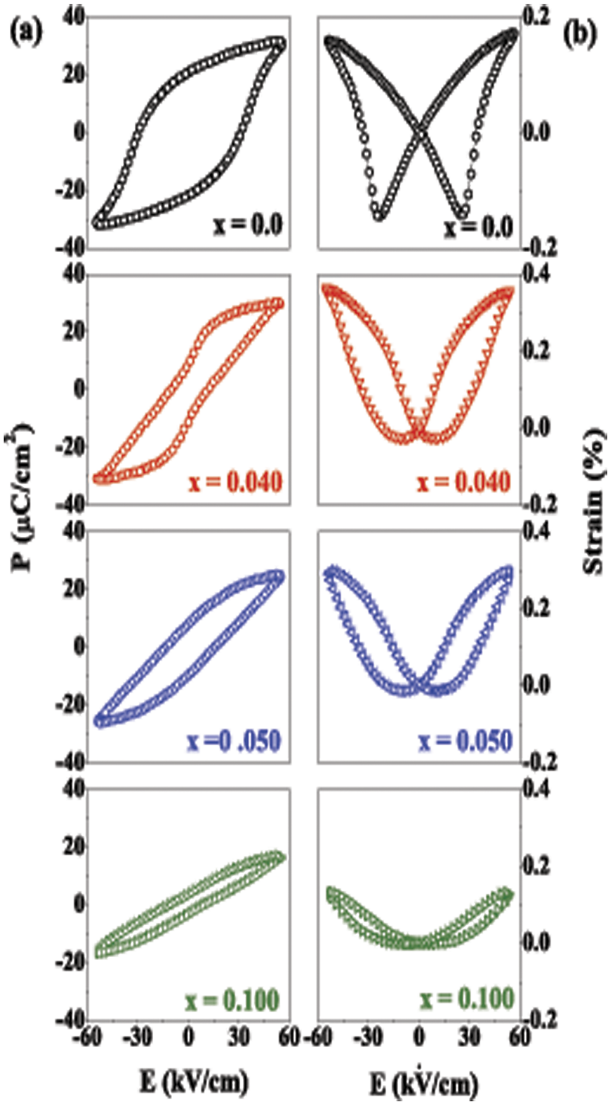

FIG. 2. (a) Polarization hysteresis loops, and (b) bipolar strain curves of $(1 - x)$BNKT-xBNiT (x = 0.0, 0.040, 0.050, and 0.100).

($x = 0.0$) which is structurally tetragonal and non-ergodic relaxor at room temperature, it exhibits typical FE hysteresis loops (square-like and butterfly-shaped for P_3-E and S_{33}-E curves, respectively). With the increase of x value ($x = 0.040$ and 0.050), pinched and sprout-shaped hysteresis loops emerge in the P_3-E and S_{33}-E characteristics due to the development of ergodicity, respectively. Note that the observed intermediate/non-equilibrium state in these hysteretic characteristics is the hallmark of the coexistence of ergodic and non-ergodic phases.[11,17,20,34–36] In BNT-based relaxor FEs, it should also be noted that the emergence of ergodicity arises from a metrically cubic phase transition.[11,18,20,32–34] It follows that the $(1 - x)$BNKT-xBNiT ceramics with the particular BNiT contents of 0.040 and 0.050 are in the vicinity of the NR-to-ER phase transition at room temperature. Thus, it is highly plausible that the transition temperature $T_{F\text{-}R}$ is quite close to room temperature. With a more increment in the BNiT content ($x \geq 0.050$), the hysteretic nature becomes much weaker resulting in slimmer and parabolic-like in the P_3-E and S_{33}-E curves, respectively. Namely, the ceramics with these BNiT compositions lies on a metrically cubic and typical ergodic relaxor phase. In unipolar S_{33}-E measurements, a similar tendency in the hysteretic shape is observed, too (see Fig. S6 of the supplementary material).

To gain a room-temperature electrostrictive coefficient Q_{33} in our $(1-x)$BNKT-xBNiT ceramics, strain S_{33} is plotted as a function of polarization P_3 [Fig. 3(a)]. For this aim, the out-of-plane S_{33} and P_3 were simultaneously measured at room temperature under a triangular electric-field wave with the frequency of 1 Hz using the aixACCT Ceramic Multilayer Actuator (aixCMA) test bench.[11] It should be emphasized that the S_{33} is linearly proportional to the $P_3{}^2$ with no hysteretic property for the only two samples with the BNiT concentrations $x = 0.040$ and 0.050 in the proximity of a NR-to-ER phase transition. For other ceramics with different BNiT concentrations ($x = 0.0$, 0.015, and 0.030), the hysteretic nature still remains in the S_{33}-$P_3{}^2$ curves, which means that the eletrostrictive responses are not pure [Fig. 3(a)]. Considering the fact that $Q_{33} = S_{33}/P_3{}^2$, for the only two samples with the BNiT concentrations of $x = 0.040$ and 0.050, the high electrostrictive coefficients of 0.025 and 0.030 m^4/C^2 are attributed to the large electromechanical strain of 0.36% and 0.30% and the relatively small polarization of 10 and 8 $\mu C/cm^2$, respectively (see Fig. S7 of the supplementary material). For the ceramics with higher BNiT contents (0.060, 0.075, and 0.100), the Q_{33} would become smaller due to the small strain values (0.1% ~ 0.2%) (see Fig. S6 of the supplementary material). It follows that the sizeable increase of the Q_{33} in the $(1-x)$BNKT-xBNiT ceramics ($x = 0.040$ and 0.050) originates from the enhancement of the S_{33} and the reduction of the P_3.

BNKT-BNiT compounds could be a promising candidate offering the possibility for new electromechanical devices due to the giant room-temperature electrostrictive coefficient Q_{33}. A comparison of the room-temperature Q_{33} values with those in other lead-based and lead-free BNT-based electrostrictive materials shows that the highest value is achieved in our $(1-x)$BNKT-xBNiT ceramics [Fig. 3(b)].[4,8,10–14,34,37–42] For the $(1-x)$BNKT-xBNiT sample with $x = 0.050$, the Q_{33} value increases up to 0.030 m^4/C^2. It is worthy of noting the reported Q_{33} values of lead-based materials such as PMN (~0.023 m^4/C^2), PZT (~0.021 m^4/C^2), PLZT (~0.015 m^4/C^2), PMN crystal (~0.025 m^4/C^2), and PZN crystal (~0.023 m^4/C^2).[37–42] We also found that the attained Q_{33} values are insensitive to temperature variations (i.e., stable for thermal fluctuations) (Fig. 4). In the temperature range between 30 and 150 °C, the S_{33}-$P_3{}^2$ curves were measured in two $(1-x)$BNKT-xBNiT ceramics ($x = 0.040$ and 0.050). It is evident that there is no hysteretic features in the S_{33}-$P_3{}^2$ curves except for that measured at 150 °C [Figs. 4(a) and 4(b)] and further, the derived electrostrictive coefficients Q_{33} are independent of the temperature with finite values close to 0.025 and 0.030 m^4/C^2 ($x = 0.040$ and 0.050, respectively) [Fig. 4(c)]. Thus, it is highly likely that our BNKT-BNiT compounds are used for the potential applications as micro-devices (e.g., actuator)

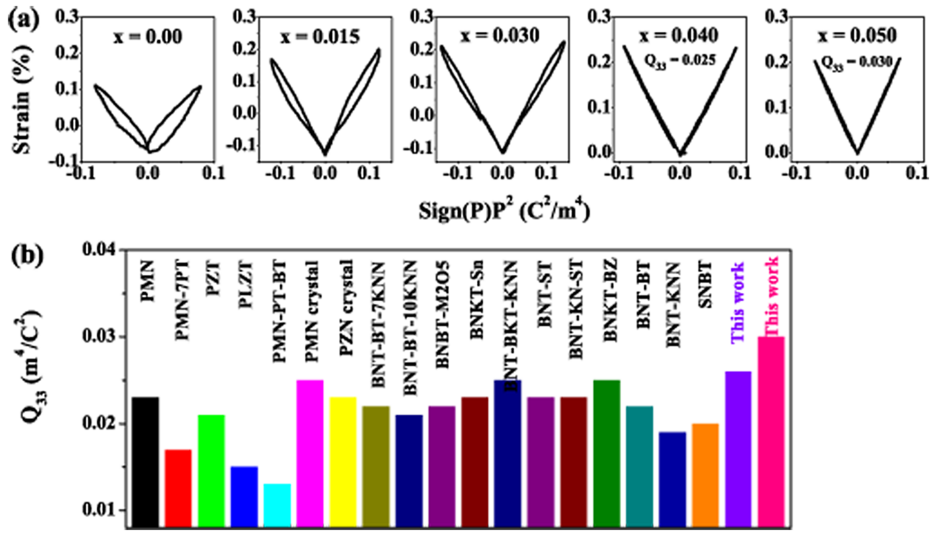

FIG. 3. Room temperature S-P^2 curves of the $(1-x)$BNKT-xBNiT (a) $x = 0.0$, 0.015, 0.030, 0.040, and 0.050, (b) comparison of electrostrictive coefficients Q_{33} of the present system with traditional lead-based and lead-free relaxor BNT-based materials.

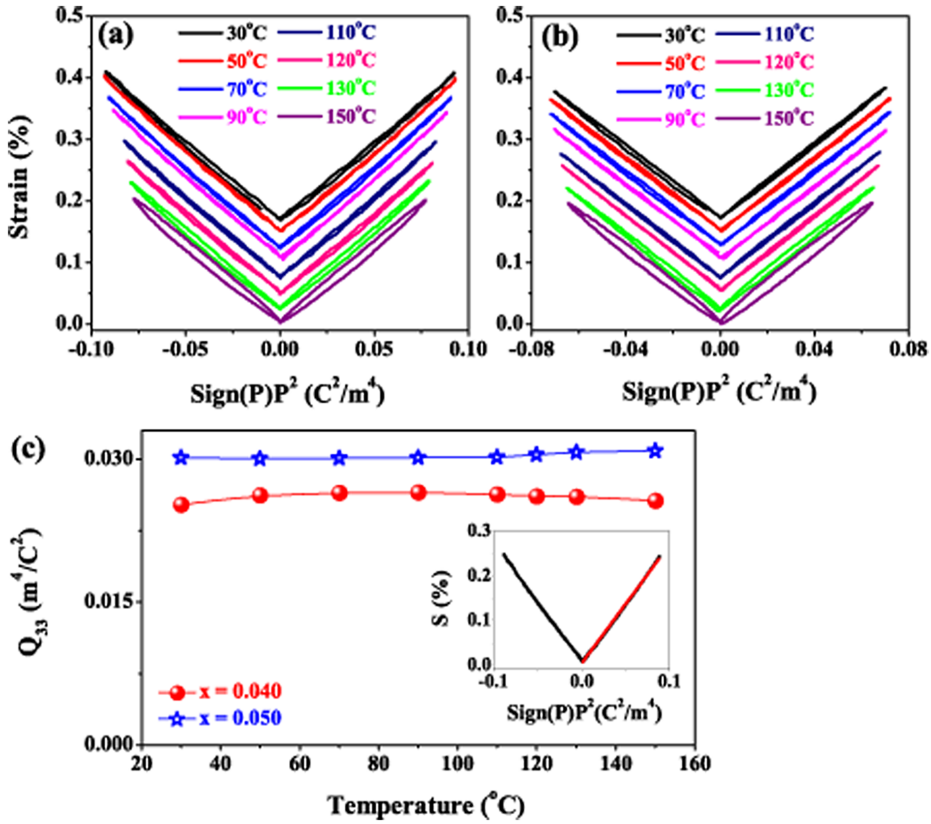

FIG. 4. Temperature-dependent S-P^2 curves of the representative compositions: (a) x = 0.040 and (b) x = 0.050, (c) temperature-dependent electrostrictive coefficients Q_{33} of the representative compositions x = 0.040 and 0.050.

where high electrostrictive coefficient and robust thermal durability are required around room temperature.

In summary, a large room-temperature electrostrictive coefficient of 0.030 m^4/C^2 is attained in BNT-based relaxor ferroelectrics, as the direct product of the compositionally-driven shift of the thermotropic phase boundary between non-ergodic and ergodic phases. With the giant electrostrictive responses, we firmly believe that the lead-free BNKT-BNiT compounds are applicable for the biocompatible utilizations, enabling the realization of novel MEMS devices with a high performance at room temperature.

See supplementary material for the additional detail regarding experimental procedure, schematic diagram of electrostrictive coefficient, microstructural analysis, XRD study, schematic representation of crystallographic phases, XPS study, unipolar *S-E* loop, and summary of phase diagram.

This work was supported by Brain Pool Program through the Korean Federation of Science and Technology Societies (KOFST) grant funded by the Ministry of Science, ICT and Future Planning (No. 172S-1-3-1900). The authors would also like to acknowledge the National Research Foundation of Korea (NRF) grants funded by the Korea government (Ministry of Education) (No. 2017R1D1A1B03028614) and (No. 2017R1D1A1B03036032) and Priority Research Centers Program through the National Research Foundation of Korea (NRF) funded by the Ministry of Education (No. 2009-0093818).

[1] G. H. Haertling, J. Am. Ceram. Soc. **82**, 797 (1999).
[2] S. E. Park and T. R. Shrout, J. Appl. Phys. **82**, 1804 (1997).
[3] J. Rodel, W. Jo, K. T. P. Seifert, E. M. Anton, T. Granzow, and D. Damjanovic, J. Am. Ceram. Soc. **92**, 1153–1177 (2009).
[4] C. Ang and Z. Yu, Adv. Mater. **18**, 103 (2006).
[5] B. E. Vugmeister, Phys. Rev. B **73**, 174117 (2006).
[6] E. M. Sabolsky, S. Trolier-McKinstry, and G. L. Messing, J. Appl. Phys. **93**, 4072 (2003).

[7] S. E. Park and T. R. Shrout, IEEE Trans. Ultrason., Ferroelectr. Freq. Control **44**, 1140 (1997).
[8] S. T. Zhang, A. B. Kounga, W. Jo, C. Jamin, K. Seifert, T. Granzow, J. Rodel, and D. Damjanovic, Adv. Mater. **21**, 4716 (2009).
[9] S. T. Zhang, F. Yan, B. Yang, and W. Cao, Appl. Phys. Lett. **97**, 122901 (2010).
[10] W. Bai, L. Li, W. Wang, B. Shen, and J. Zhai, Solid State Commun. **206**, 22 (2015).
[11] H. S. Han, W. Jo, J. K. Kang, C. W. Ahn, I. W. Kim, K. K. Ahn, and J. S. Lee, J. Appl. Phys. **113**, 154102 (2013).
[12] J. Hao, Z. Xu, R. Chu, W. Li, P. Fu, J. Du, and G. Li, J. Eur. Ceram. Soc. **36**, 4003 (2016).
[13] F. Wang, C. Jin, Q. Yao, and W. Shi, J. Appl. Phys. **114**, 027004 (2013).
[14] J. Hao, Z. Xu, R. Chu, W. Li, and J. Du, J. Mater. Sci. **50**, 5328 (2015).
[15] C. W. Ahn, G. H. Choi, I. W. Kim, J. S. Lee, K. Wang, Y. Hwang, and W. Jo, NPG Asia Mater. **9**, e346 (2017).
[16] C. H. Hong, H. P. Kim, B. Y. Choi, H. S. Han, J. S. Son, C. W. Ahn, and W. Jo, J. Materiomics **2**, 1–24 (2016).
[17] W. Jo, R. Dittmer, M. Acosta, J. Zang, C. Groh, E. Sapper, K. Wang, and J. Rödel, J. Electroceram. **29**, 71 (2012).
[18] A. Ullah, C. W. Ahn, A. Ullah, and I. W. Kim, Appl. Phys. Lett. **103**, 022906 (2013).
[19] J. Shi, H. Fan, X. Liu, and A. J. Bell, J. Am. Ceram. Soc. **97**, 848 (2014).
[20] A. Ullah, C. W. Ahn, A. Hussain, S. Y. Lee, and I. W. Kim, J. Am. Ceram. Soc. **94**, 3915 (2011).
[21] S. G. Lu, Z. Xu, and H. Chen, Phys. Rev. B **72**, 054120 (2005).
[22] A. Ullah, C. W. Ahn, A. Hussain, S. Y. Lee, H. J. Lee, and I. W. Kim, Curr. Appl. Phys. **10**, 1174 (2010).
[23] T. Qi, I. Grinberg, and A. M. Rappe, Phys. Rev. B **79**, 094114 (2009).
[24] W. Bai, F. Liu, P. Li, B. Shen, J. Zhai, and H. Chen, J. Eur. Ceram. Soc. **35**, 3457 (2015).
[25] J. Hao, B. Shen, J. Zhai, C. Liu, X. Li, and X. Gao, J. Appl. Phys. **113**, 114106 (2013).
[26] R. E. Cohen, Nature **358**, 136 (1992).
[27] P. Hu, J. Chen, J. Deng, and X. Xing, J. Am. Chem. Soc. **132**, 1925 (2010).
[28] C. Fu, N. Chen, and G. Du, Ceram. Int. **43**, 15927 (2017).
[29] Q. Xu, W. Chen, and R. Yuan, J. Mater. Sci. Technol. **17**, 535 (2001).
[30] H. A. Loytty, M. W. Louie, M. R. Singh, L. Li, H. G. S. Casalongue, H. Ogasawara, E. J. Crumlin, Z. Liu, A. T. Bell, A. Nilsson, and D. Friebel, J. Phys. Chem. C **120**, 2247 (2016).
[31] H. W. Nesbitt, D. Legrand, and G. M. Bancroft, Phys. Chem. Miner. **27**, 357 (2000).
[32] N. Kumar and D. P. Cann, J. Appl. Phys. **114**, 054102 (2013).
[33] J. Hao, W. Bai, W. Li, B. Shen, and J. Zhai, J. Appl. Phys. **114**, 044103 (2013).
[34] J. Hao, W. Bai, W. Li, B. Shen, and J. Zhai, J. Mater. Res. **27**, 2943 (2012).
[35] W. Bai, D. Chen, P. Zheng, B. Shen, J. Zhai, and Z. Ji, Dalton Trans. **45**, 8573 (2016).
[36] W. Bai, B. Shen, J. Zhai, F. Liu, P. Li, B. Liu, and Y. Zhang, Dalton Trans. **45**, 14141 (2016).
[37] J. Kuwata, K. Uchino, and S. Nomura, Jpn. J. Appl. Phys., Part I **19**, 2099 (1980).
[38] G. H. Haertling, Ferroelectrics **75**, 25 (1987).
[39] P. M. Weaver, M. G. Cain, and M. Stewart, Appl. Phys. Lett. **96**, 142905 (2010).
[40] M. B. Rauls, W. Dong, J. E. Huber, and C. S. Lynch, Acta Mater. **59**, 2713 (2011).
[41] L. Jin, R. Huo, R. Guo, F. Li, D. Wang, Y. Tian, Q. Hu, X. Wei, Z. He, Y. Yan, and G. Liu, ACS Appl. Mater. Interface **8**, 31109 (2016).
[42] C. B. Diantonio, F. A. Williams, and S. M. Pilgrim, IEEE Trans. Ultrason., Ferroelectr. Freq. Control **48**, 1532 (2001).